

# Search for $2\beta$ decay of Zinc and Tungsten with the help of low-background $\text{ZnWO}_4$ crystal scintillators

P. Belli<sup>a</sup>, R. Bernabei<sup>a,1</sup>, F. Cappella<sup>b</sup>, R. Cerulli<sup>c</sup>, F.A. Danevich<sup>d</sup>, B.V. Grinyov<sup>e</sup>, A. Incicchitti<sup>b</sup>, V.V. Kobychiev<sup>d</sup>, V.M. Mokina<sup>d</sup>, S.S. Nagorny<sup>d</sup>, L.L. Nagornaya<sup>e</sup>, S. Nisi<sup>c</sup>, F. Nozzoli<sup>a</sup>, D.V. Poda<sup>d</sup>, D. Prosperi<sup>b</sup>, V.I. Tretyak<sup>d</sup>, S.S. Yurchenko<sup>d</sup>

<sup>a</sup>*Dipartimento di Fisica, Università di Roma “Tor Vergata” and INFN, Sezione di Roma Tor Vergata, I-00133 Rome, Italy*

<sup>b</sup>*Dipartimento di Fisica, Università di Roma “La Sapienza” and INFN, Sezione di Roma, I-00185 Rome, Italy*

<sup>c</sup>*INFN, Laboratori Nazionali del Gran Sasso, 67010 Assergi (AQ), Italy*

<sup>d</sup>*Institute for Nuclear Research, MSP 03680 Kyiv, Ukraine*

<sup>e</sup>*Institute for Scintillation Materials, 61001 Kharkiv, Ukraine*

## Abstract

Double beta processes in  $^{64}\text{Zn}$ ,  $^{70}\text{Zn}$ ,  $^{180}\text{W}$ , and  $^{186}\text{W}$  have been searched for with the help of large volume (0.1 – 0.7 kg) low background  $\text{ZnWO}_4$  crystal scintillators at the Gran Sasso National Laboratories of the INFN. Total time of measurements exceeds 10 thousands hours. New improved half-life limits on double electron capture and electron capture with positron emission in  $^{64}\text{Zn}$  have been set, in particular (all the limits are at 90% C.L.):  $T_{1/2}^{0\nu 2\varepsilon} \geq 1.1 \times 10^{20}$  yr,  $T_{1/2}^{2\nu\varepsilon\beta^+} \geq 7.0 \times 10^{20}$  yr, and  $T_{1/2}^{0\nu\varepsilon\beta^+} \geq 4.3 \times 10^{20}$  yr. The different modes of  $2\beta$  processes in  $^{70}\text{Zn}$ ,  $^{180}\text{W}$ , and  $^{186}\text{W}$  have been restricted at the level of  $10^{17} - 10^{20}$  yr.

*PACS:* 29.40.Mc, 23.40.-s

*Keywords:* Double beta decay;  $^{64}\text{Zn}$ ;  $^{70}\text{Zn}$ ;  $^{180}\text{W}$ ;  $^{186}\text{W}$ ;  $\text{ZnWO}_4$  crystal scintillators

## 1 Introduction

Neutrinoless ( $0\nu$ ) double beta ( $2\beta$ ) decay is one of the low-energy effects which are forbidden in the Standard Model (SM) because of violation of the lepton number on two units. However, it is naturally expected in many SM extensions.  $0\nu 2\beta$  experiments offer complementary information to those given by neutrino oscillation experiments. While oscillation experiments are sensitive to the neutrino mass differences, the  $0\nu 2\beta$  decay rate could determine an absolute scale of neutrino mass, and the neutrino mass hierarchy. Besides, double beta decay experiments allow to prove the nature of neutrino (that is, if it is a Majorana particle,  $\nu = \bar{\nu}$ , or a Dirac particle,

---

<sup>1</sup>Corresponding author. *E-mail address:* rita.bernabei@roma2.infn.it (R. Bernabei)

$\nu \neq \bar{\nu}$ ), existence of right-handed admixtures in weak interaction, and to test a range of other effects beyond the SM [1, 2, 3, 4, 5, 6, 7, 8, 9].

Experimental investigations in this field are concentrated mostly on  $2\beta^-$  decays, processes with emission of two electrons. Developments in the experimental techniques during the last two decades lead to observation of the two neutrino ( $2\nu$ )  $2\beta^-$  decay in 10 isotopes with half-lives in the range of  $10^{18} - 10^{21}$  yr, and to impressive improvement of sensitivity to the neutrinoless mode of  $2\beta^-$  decay up to  $10^{23} - 10^{25}$  yr [1].

Results for double positron decay ( $2\beta^+$ ), electron capture with positron emission ( $\varepsilon\beta^+$ ), and capture of two electrons from atomic shells ( $2\varepsilon$ ) are much more modest. The most sensitive experiments give the limits on the  $2\varepsilon$ ,  $\varepsilon\beta^+$  and  $2\beta^+$  processes on the level of  $10^{17} - 10^{21}$  yr [1]. Reasons for such a situation are: (1) lower energy releases in  $2\varepsilon$ ,  $\varepsilon\beta^+$  and  $2\beta^+$  processes in comparison with those in  $2\beta^-$  decay, that results in higher expected  $T_{1/2}$  values, as well as provides difficulties to suppress background; (2) usually lower natural abundances of  $2\beta^+$  isotopes (which are typically lower than 1% with only few exceptions). Nevertheless, studies of  $\varepsilon\beta^+$  and  $2\varepsilon$  decays could help to distinguish the mechanism of neutrinoless  $2\beta$  decay (is it due to non-zero neutrino mass or to the right-handed admixtures in weak interactions) [10].

$^{64}\text{Zn}$  is one of a few exceptions among  $2\beta^+$  nuclei having big natural isotopic abundance (see Table 1 where properties of potentially  $2\beta$  active nuclides present in zinc tungstate ( $\text{ZnWO}_4$ ) crystals are listed). This feature allows to build a large scale experiment without expensive isotopical enrichment. With the mass difference between  $^{64}\text{Zn}$  and  $^{64}\text{Ni}$  nuclei of 1095.7 keV [11], double electron capture and electron capture with emission of positron are energetically allowed.

Table 1: Potentially  $2\beta$  active nuclides present in  $\text{ZnWO}_4$  crystals.

Transition	Energy release (keV) [11]	Isotopic abundance (%) [12]	Decay channels	Number of nuclei in 100 g of $\text{ZnWO}_4$ crystal
$^{64}\text{Zn} \rightarrow ^{64}\text{Ni}$	1095.7(0.7)	48.268(0.321)	$2\varepsilon, \varepsilon\beta^+$	$9.28 \times 10^{22}$
$^{70}\text{Zn} \rightarrow ^{70}\text{Ge}$	998.5(2.2)	0.631(0.009)	$2\beta^-$	$1.21 \times 10^{21}$
$^{180}\text{W} \rightarrow ^{180}\text{Hf}$	144(4)	0.12(0.01)	$2\varepsilon$	$2.31 \times 10^{20}$
$^{186}\text{W} \rightarrow ^{186}\text{Os}$	489.9(1.4)	28.43(0.19)	$2\beta^-$	$5.47 \times 10^{22}$

A possible experimental indication of the  $\varepsilon\beta^+$  decay of  $^{64}\text{Zn}$  with  $T_{1/2}^{(0\nu+2\nu)\varepsilon\beta^+} = (1.1 \pm 0.9) \times 10^{19}$  yr was suggested in Ref. [13]. A  $\varnothing 7.6 \times 7.6$  cm NaI(Tl) scintillator and a 25% efficiency HP Ge detector, operating in coincidence, were used in that experiment. The excess of  $\approx 85$  events in the 511 keV peak was observed with Zinc sample (mass of 350 g, 392 h of exposure on the sea level), while no effect was detected without sample or with Copper or Iron blanks.

During last decade sensitivities of other experiments were not enough to confirm or disprove the result of Ref. [13]. CdZnTe semiconductor detector was used to search for  $2\beta$  decays of  $^{64}\text{Zn}$  in underground measurements performed in the Gran Sasso National Laboratories (LNGS, depth of  $\simeq 3600$  m w.e.) during 1117 h in the COBRA experiment; however, small mass of the detector (near 3 g) allowed to reach half-life limits at the level of  $10^{16} - 10^{17}$  yr [14]. Low-background experiment with  $\text{ZnWO}_4$  crystal scintillator was performed in the Solotvina Underground Laboratory ( $\simeq 1000$  m w.e.) [15]. Despite the low mass of the detector (4.5 g)

and short time of the measurements (429 h), limits at level of  $10^{18}$  yr were set for  $2\beta$  processes in  $^{64}\text{Zn}$ .

In the experiment [16] two detectors, HP Ge 456 cm<sup>3</sup> and CsI(Tl)  $\simeq 400$  cm<sup>3</sup>, were used in coincidence in measurements with 460 g Zn sample in the underground Cheong Pyung Laboratory ( $\simeq 1000$  m w.e.). Measurements during 375 h gave the limit on  $\varepsilon\beta^+$  decay of  $^{64}\text{Zn}$  as:  $T_{1/2}^{(0\nu+2\nu)\varepsilon\beta^+} > 1.3 \times 10^{20}$  yr. Further improvement of sensitivity was reached at the first stage [17] of the experiment presented here. The measurements were performed in the LNGS with the help of large  $\text{ZnWO}_4$  scintillator (mass of 117 g) over 1902 h. New improved half-life limits on  $2\nu$  and  $0\nu$   $\varepsilon\beta^+$  decay of  $^{64}\text{Zn}$  were established as:  $T_{1/2}^{2\nu\varepsilon\beta^+} \geq 2.1 \times 10^{20}$  yr,  $T_{1/2}^{0\nu\varepsilon\beta^+} \geq 2.2 \times 10^{20}$  yr [17]. New limits on different modes of double electron capture in  $^{64}\text{Zn}$  have been obtained too:  $T_{1/2}^{2\nu 2K} \geq 6.2 \times 10^{18}$  yr,  $T_{1/2}^{0\nu 2K} \geq 4.0 \times 10^{18}$  yr, and  $T_{1/2}^{0\nu 2\varepsilon} \geq 3.4 \times 10^{18}$  yr, all at 90% C.L. [17].

In addition to  $^{64}\text{Zn}$ ,  $\text{ZnWO}_4$  scintillators contain a few other potentially  $2\beta$  active isotopes:  $^{70}\text{Zn}$ ,  $^{180}\text{W}$  and  $^{186}\text{W}$  (see Table 1). The best up to date half-life limits on different modes and channels of  $2\beta$  processes in these isotopes were obtained in low-background measurements carried out in the Solotvina Underground Laboratory ( $\simeq 1000$  m w.e.) with  $\text{ZnWO}_4$  and  $\text{CdWO}_4$  crystal scintillators. The half-life limits of  $2\beta^-$  decay of  $^{70}\text{Zn}$ :  $T_{1/2}^{2\nu 2\beta^-} \geq 1.3 \times 10^{16}$  yr, and  $T_{1/2}^{0\nu 2\beta^-} \geq 0.7 \times 10^{18}$  yr at 90% C.L. were set in the work [15]. The data accumulated over 13316 h with 330 g  $\text{CdWO}_4$  detector enriched in  $^{116}\text{Cd}$  were analyzed to search for  $2\beta$  decay of  $^{186}\text{W}$  at the level of  $T_{1/2}^{2\nu 2\beta^-} (^{186}\text{W}) \geq 3.7 \times 10^{18}$  yr,  $T_{1/2}^{0\nu 2\beta^-} (^{186}\text{W}) \geq 1.1 \times 10^{21}$  yr (all at 90% C.L.) [18]. Data of 692 h of the measurements with low energy threshold were taken to set the following limits on the double electron capture in  $^{180}\text{W}$ :  $T_{1/2}^{2\nu 2K} (^{180}\text{W}) \geq 0.7 \times 10^{17}$  yr,  $T_{1/2}^{0\nu 2\varepsilon} (^{180}\text{W}) \geq 0.9 \times 10^{17}$  yr.

These experiments have demonstrated a good potential of  $\text{ZnWO}_4$  (and  $\text{CdWO}_4$ ) scintillators to search for double beta processes in Zinc and Tungsten isotopes. The main properties of  $\text{ZnWO}_4$  scintillators are: (i) density equal to 7.8 g/cm<sup>3</sup>; (ii) light yield  $\simeq 13\%$  of that of NaI(Tl); (iii) refractive index equal to 2.1–2.2; (iv) emission maximum at 480 nm; (v) effective average decay time is 24  $\mu\text{s}$  (at room temperature). The material is non-hygroscopic and chemically inert; the melting point is at 1200 °C. Radiopurity of zinc tungstate crystals has been preliminary investigated in [15]. Development of large volume high scintillation properties low-background  $\text{ZnWO}_4$  crystal scintillators was realized recently [19, 20].

Aim of the present work is to search for  $2\varepsilon$  capture and  $\varepsilon\beta^+$  decay of  $^{64}\text{Zn}$  with the help of large low-background  $\text{ZnWO}_4$  crystal scintillators. In addition, search for double beta decays of  $^{70}\text{Zn}$ ,  $^{180}\text{W}$ , and  $^{186}\text{W}$  have been realized as by-products of the experiment.

## 2 Measurements

### 2.1 Detector

Two clear, slightly pink colored  $\text{ZnWO}_4$  crystals produced from single crystals grown by the Czochralski method were used in our experiment. Two batches of zinc oxide from different producers were used to prepare  $\text{ZnWO}_4$  compounds for the crystal growth. The crystals used for measurements are listed in Table 2. The third scintillator (ZWO-2a) was cut from the large 0.7 kg crystal (ZWO-2).

Table 2: ZnWO<sub>4</sub> crystal scintillators used in the present experiments.

Crystal scintillator	Size (mm)	Mass (g)
ZWO-1	20 × 19 × 40	117
ZWO-2	∅44 × 55	699
ZWO-2a	∅44 × 14	168

The ZnWO<sub>4</sub> crystals were fixed inside a cavity of ∅47 × 59 mm in the central part of a polystyrene light-guide 66 mm in diameter and 312 mm in length. The cavity was filled up with high-pure silicon oil. The light-guide was optically connected on opposite sides by optical couplant to two low radioactive EMI9265–B53/FL 3” photomultipliers (PMT). The light-guide was wrapped by PTFE reflection tape.

The detector has been installed deep underground ( $\simeq 3600$  m w.e.) in the low background DAMA/R&D set-up at the LNGS. It was surrounded by Cu bricks and sealed in a low radioactive air-tight Cu box continuously flushed with high purity nitrogen gas (stored deeply underground for a long time) to avoid presence of residual environmental Radon. The Cu box has been surrounded by a passive shield made of 10 cm of high purity Cu, 15 cm of low radioactive lead, 1.5 mm of cadmium and 4/10 cm polyethylene/paraffin to reduce the external background. The whole shield has been closed inside a Plexiglas box, also continuously flushed by high purity nitrogen gas.

An event-by-event data acquisition system records the amplitude and the arrival time of the events. Moreover, the sum of the signals from the PMTs was also recorded by a 1 GS/s 8 bit DC270 Transient Digitizer by Acqiris over a time window of 100  $\mu$ s. To allow a good compromise to handle the data files and taking into account the slow scintillation decay of ZnWO<sub>4</sub>, 20 MS/s sampling frequency was used during the data taking.

## 2.2 Low-background measurements

The experiment was realized in the LNGS at a depth of 3600 m w.e. The measurements were carried out in four runs (see Table 3 for details). The data of Run 1 have been already analyzed and published in [17].

The energy scale and resolution of the ZnWO<sub>4</sub> detectors have been measured with <sup>22</sup>Na, <sup>133</sup>Ba, <sup>137</sup>Cs, <sup>228</sup>Th and <sup>241</sup>Am  $\gamma$  sources. Dependence of energy resolution of the ZnWO<sub>4</sub> detectors on energy can be fitted by the function:  $\text{FWHM}_\gamma(\text{keV}) = \sqrt{a + b \cdot E_\gamma}$ , where  $E_\gamma$  is the energy of  $\gamma$  quanta in keV. For instance, the calibration energy spectra accumulated with <sup>133</sup>Ba, <sup>137</sup>Cs and <sup>241</sup>Am in the beginning of Run 4 are shown in Fig. 1. The values of parameters  $a$  and  $b$  for the Run 4 are  $a = 190(40)$  keV<sup>2</sup> and  $b = 7.34(35)$  keV. The energy resolutions measured with the ZnWO<sub>4</sub> detectors for 662 keV  $\gamma$  quanta of <sup>137</sup>Cs are presented in Table 3.

The energy spectra measured with the ZnWO<sub>4</sub> detectors (ZWO-1 and ZWO-2) in the low-background set-up are presented in Fig. 2. The spectra are normalized on the mass of the crystals and time of the measurements. A few peaks in the spectra can be ascribed to  $\gamma$  quanta of naturally occurred radionuclides <sup>40</sup>K, <sup>214</sup>Bi (<sup>238</sup>U chain) and <sup>208</sup>Tl (<sup>232</sup>Th) from materials

Table 3: Description of low-background measurements with  $\text{ZnWO}_4$  crystal scintillators. Time of measurements ( $t$ ), energy interval of data taking ( $\Delta E$ ), energy resolutions at 662 keV  $\gamma$  line of  $^{137}\text{Cs}$  (FWHM), and background counting rates in different energy intervals are specified.

Run	Crystal scintillator	$t$ (h)	$\Delta E$ (MeV)	FWHM (%)	Rate (counts/day/keV/kg) in energy interval (MeV)			
					0.2–0.4	0.8–1.0	2.0–2.9	3.0–4.0
1	ZWO-1	1902	0.01–1	11.5	1.93(3)	0.27(1)		
2	ZWO-1	2906	0.05–4	12.6	1.71(2)	0.25(1)	0.0072(7)	0.0003(1)
3	ZWO-2	2130	0.05–4	14.6	1.07(1)	0.149(3)	0.0072(4)	0.00031(7)
4	ZWO-2a	3292	0.01–1	11.0	1.52(2)	0.211(7)		

of the set-up (we suppose the PMTs as the main sources of the  $\gamma$  background). Some part of the background counting rate is due to internal radioactive contamination of the crystals. Background counting rates in the energy intervals 0.2 – 0.4, 0.8 – 1.0, 2.0 – 2.9, and 3.0 – 4.0 MeV are presented in Table 3. The background of the detectors will be analyzed in section 3.

### 2.3 Mass spectrometric measurements of the impurities in the $\text{ZnWO}_4$ crystals

In order to estimate the presence of naturally occurring radioactive isotopes, the  $\text{ZnWO}_4$  crystals were measured with the help of Inductively Coupled Plasma - Mass Spectrometry (ICP-MS, Agilent Technologies model 7500a) at the LNGS.

Samples of the  $\text{ZnWO}_4$  crystals (ZWO-1 and ZWO-2) were reduced to powder by mechanical treatment inside a clean polyethylene bag to avoid possible external contamination. The samples were etched in a microwave assisted acid digestion technique (Method EPA 3052) using nitric acid and nitric-hydrofluoric acid mixtures. The results for both procedures were just a partial sample dissolution. The solutions obtained after centrifugation have been analyzed by ICP-MS.

The measurements have been carried out in semiquantitative mode. The instrumentation was calibrated with the help of a single solution containing 10 ppb of Li, Co, Y, Ce, and Tl. The results of the measurements of the  $\text{ZnWO}_4$  samples are presented in Table 4. The accuracy of the measurements are on the level of 20–30%. However, the errors for some elements could be higher. In particular, in a case of Th interference with tungsten oxide  $^{184}\text{W}^{16}\text{O}_3$  can lead to considerable ambiguity. Indeed the measured contamination of the crystal ZWO-1 by thorium on the level of 25 ppb corresponds to activity of  $^{232}\text{Th} \approx 0.1$  Bq/kg. As it will be shown in section 3.1, the  $^{232}\text{Th}$  contamination in the crystal ZWO-1, determined by analysis of data of the low-background measurements, is much lower.

## 3 Background of $\text{ZnWO}_4$ detectors

Knowledge of the radioactive contamination of the  $\text{ZnWO}_4$  crystals is necessary to describe the background in the energy intervals of the  $2\beta$  processes in Zn and W. The time-amplitude anal-

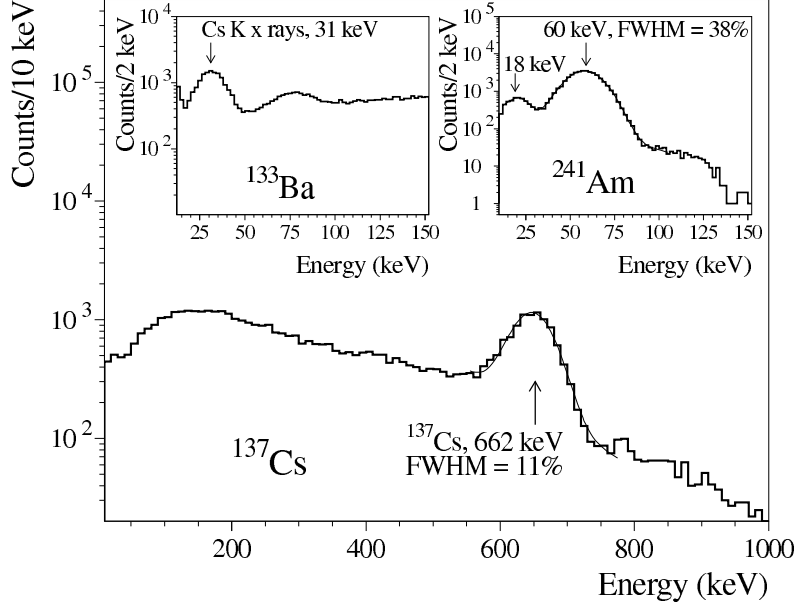


Figure 1: Energy spectra measured by ZnWO<sub>4</sub> detector (ZWO-2a) with <sup>137</sup>Cs (main part), <sup>133</sup>Ba and <sup>241</sup>Am (inserts)  $\gamma$  sources.

ysis, the pulse-shape discrimination, and the Monte Carlo simulation were applied in addition to the ICP-MS measurements to reconstruct the measured background spectra of the ZnWO<sub>4</sub> detectors, and to estimate their radioactive contamination.

### 3.1 Time-amplitude analysis

The activity of <sup>228</sup>Th (<sup>232</sup>Th family) in the ZnWO<sub>4</sub> crystals was determined with the help of the time-amplitude analysis<sup>2</sup> using the data of Run 2 and Run 3. The arrival time and the energy of events were used to select the following fast decay chain in the <sup>232</sup>Th family: <sup>224</sup>Ra ( $Q_\alpha = 5.79$  MeV)  $\rightarrow$  <sup>220</sup>Rn ( $Q_\alpha = 6.41$  MeV,  $T_{1/2} = 55.6$  s)  $\rightarrow$  <sup>216</sup>Po ( $Q_\alpha = 6.91$  MeV,  $T_{1/2} = 0.145$  s)  $\rightarrow$  <sup>212</sup>Pb.  $\alpha$  particles in ZnWO<sub>4</sub> scintillators produce a substantially lower scintillation in comparison with  $\gamma$  quanta ( $\beta$  particles). Numerically this quenching can be expressed through the  $\alpha/\beta$  ratio<sup>3</sup>. We have used the following energy dependence of the  $\alpha/\beta$  ratio derived from the measurements [15]:  $\alpha/\beta = 0.074(16) + 0.0164(40) \times E_\alpha$ , where  $E_\alpha$  is the energy of  $\alpha$  particles in MeV ( $E_\alpha > 2$  MeV).

Four and seven events of the fast chain <sup>224</sup>Ra  $\rightarrow$  <sup>220</sup>Rn  $\rightarrow$  <sup>216</sup>Po  $\rightarrow$  <sup>212</sup>Pb were found in the data of Run 2 and Run 3, respectively. Taking into account the efficiency of the events selection (65%) one can calculate the activities of <sup>228</sup>Th in the ZnWO<sub>4</sub> crystals as 5(3)  $\mu$ Bq/kg (ZWO-1) and 1.5(6)  $\mu$ Bq/kg (ZWO-2).

Similarly the limits on activity of <sup>227</sup>Ac (<sup>235</sup>U family) in the crystals was set by selection of the fast decays <sup>219</sup>Rn ( $Q_\alpha = 6.95$  MeV,  $T_{1/2} = 3.96$  s)  $\rightarrow$  <sup>215</sup>Po ( $Q_\alpha = 7.53$  MeV,  $T_{1/2} = 1.78$

<sup>2</sup>The technique of the time-amplitude analysis is described in detail in [21, 22].

<sup>3</sup>The  $\alpha/\beta$  ratio is defined as ratio of  $\alpha$  peak position in the energy scale measured with  $\gamma$  sources to the energy of  $\alpha$  particles ( $E_\alpha$ ). Because  $\gamma$  quanta interact with detector by  $\beta$  particles, we use more convenient term " $\alpha/\beta$ " ratio.

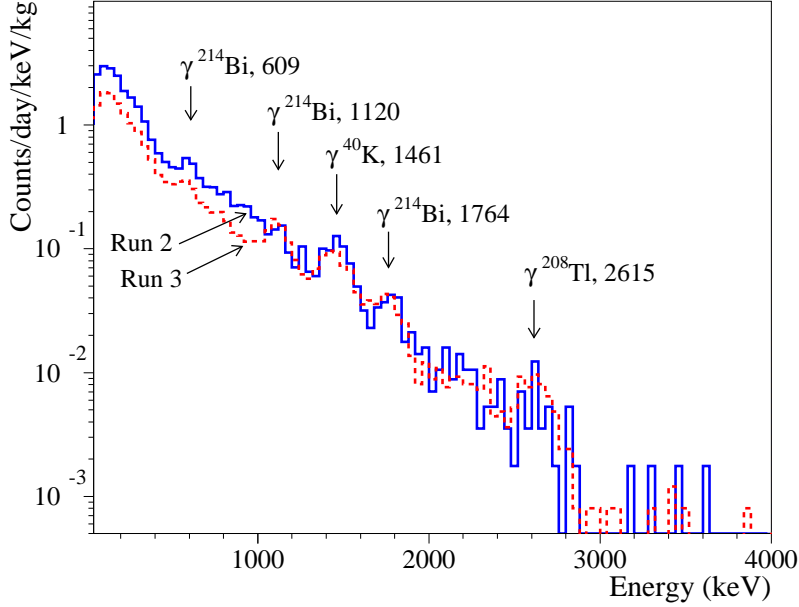


Figure 2: (Color online) Energy spectra of  $\text{ZnWO}_4$  scintillators measured in the low background set-up during Run 2 with ZWO-1 (solid line) and Run 3 with ZWO-2 (dashed line). Width of the energy bin is 30 keV. Energies of  $\gamma$  lines are in keV.

ms)  $\rightarrow$   $^{211}\text{Pb}$ .

The estimations of radioactive contamination of the  $\text{ZnWO}_4$  crystals by  $^{228}\text{Th}$  and  $^{227}\text{Ac}$  obtained with the help of the time-amplitude analysis are presented in Table 5.

### 3.2 Pulse-shape discrimination between $\beta(\gamma)$ and $\alpha$ particles

As it was demonstrated in [15], the difference in pulse shapes in  $\text{ZnWO}_4$  scintillator allows to discriminate  $\gamma(\beta)$  events from those induced by  $\alpha$  particles. The optimal filter method proposed by E. Gatti and F. De Martini in 1962 [23], developed in [24, 25] for  $\text{CdWO}_4$  crystal scintillators, and successfully used for different scintillation detectors:  $\text{CeF}_3$  [26],  $\text{CaWO}_4$  [27],  $\text{YAG:Nd}$  [28],  $\text{ZnWO}_4$  [15],  $\text{CaF}_2(\text{Eu})$  [29],  $\text{PbWO}_4$  [30],  $\text{CaMoO}_4$  [31] was applied for this purpose. For each signal  $f(t)$ , the numerical characteristic of its shape (shape indicator,  $SI$ ) was defined as  $SI = \sum f(t_k) \times P(t_k) / \sum f(t_k)$ , where the sum is over time channels  $k$ , starting from the origin of signal and up to  $50 \mu\text{s}$ ,  $f(t_k)$  is the digitized amplitude (at the time  $t_k$ ) of a given signal. The weight function  $P(t)$  was defined as:  $P(t) = \{f_\alpha(t) - f_\gamma(t)\} / \{f_\alpha(t) + f_\gamma(t)\}$ , where  $f_\alpha(t)$  and  $f_\gamma(t)$  are the reference pulse shapes for  $\alpha$  particles and  $\gamma$  quanta, respectively, obtained by summing up shapes of few thousands of  $\gamma$  or  $\alpha$  events. The scatter plot of the shape indicator versus energy for the low-background measurements in Run 3 is depicted in Fig. 3. The distribution of shape indicators for the events of Run 3 with the energies in the energy interval  $0.5 - 1.0 \text{ MeV}$  is depicted in Inset of Fig. 3. The population of  $\alpha$  events is clearly separated from  $\gamma(\beta)$  events.

The energy spectra of  $\gamma(\beta)$  and  $\alpha$  events selected with the help of the pulse-shape discrimination from data of Run 3 are shown in Fig. 4. As it was demonstrated in [15], the energy resolution for  $\alpha$  particles is considerably worse than that for  $\gamma$  quanta due to dependence of

Table 4: Contamination of ZnWO<sub>4</sub> crystal scintillators measured by ICP-MS analysis.

Element	Measured atomic mass	Concentration of element (ppb)		Possible interference
		ZWO-1	ZWO-2	
K	39	≤ 15000	≤ 30000	<sup>184</sup> W <sup>16</sup> O <sub>3</sub>
Ni	60	140	250	
Rb	85	1.5	3.2	
Cd	111	670	11000	
In	115	≤ 2.5	≤ 5	
Sm	147	≤ 4	≤ 8	
Pt	195	16	10	
Pb	208	≤ 10	≤ 20	
Th	232	25	≤ 2	
U	238	≤ 0.5	≤ 1	

the  $\alpha/\beta$  ratio on the direction of  $\alpha$  particles relative to the ZnWO<sub>4</sub> crystal axes. Therefore we cannot determine activity of U/Th  $\alpha$  active daughters in the crystal (equilibrium of U and Th chains is supposed to be broken). Fit of the  $\alpha$  spectra selected from the data of Run 2 and Run 3 allows to estimate only limits on activities of U/Th daughters (see Table 5). The total internal U/Th  $\alpha$  activity in the ZnWO<sub>4</sub> crystals is 0.38(5) mBq/kg (ZWO-1) and 0.18(3) mBq/kg (ZWO-2).

Search for fast decays <sup>214</sup>Bi ( $Q_\beta = 3.27$  MeV,  $T_{1/2} = 19.9$  m)  $\rightarrow$  <sup>214</sup>Po ( $Q_\alpha = 7.83$  MeV,  $T_{1/2} = 164$   $\mu$ s)  $\rightarrow$  <sup>210</sup>Pb (in equilibrium with <sup>226</sup>Ra from the <sup>238</sup>U chain) was performed with the help of pulse-shape analysis of double pulses<sup>4</sup>. It allows to estimate the activity of <sup>226</sup>Ra in the ZnWO<sub>4</sub> crystals at the level of a few  $\mu$ Bq/kg (Table 5).

### 3.3 Simulation of $\beta(\gamma)$ background

The most dangerous radionuclides, which could produce background in a ZnWO<sub>4</sub> detector (including daughters of these radionuclides), are listed in Table 5. As it was mentioned in section 2.2, radioactive contamination of the PMTs contributes to the background too. The distributions of the possible background components were simulated with the help of the GEANT4 package [32]. The initial kinematics of the particles emitted in the decay of nuclei was given by an event generator DECAY0 [33]. To estimate the contribution of the  $\beta(\gamma)$  active isotopes and of the  $\gamma$  rays from the PMTs, the measured background spectra of the ZnWO<sub>4</sub> detectors (Run 2 and Run 3), after rejection of  $\alpha$  events by the pulse-shape discrimination, were fitted by the model built from the simulated distributions. Activities of U/Th daughters in the crystals were restricted taking into account the results of the time-amplitude and pulse-shape analyzes. The activities of <sup>40</sup>K, <sup>232</sup>Th and <sup>238</sup>U inside the PMTs were taken from [34]. The peak in the spectrum of Run 3 at the energy  $\approx 1.1$  MeV cannot be explained by contribution from external  $\gamma$  rays (the 1120 keV  $\gamma$  line of <sup>214</sup>Bi is not enough intensive to provide the whole peak area). We suppose presence in the crystal of <sup>65</sup>Zn ( $T_{1/2} = 244.26$  d,  $Q_\beta = 1351.9$  keV [35]) which can

<sup>4</sup>The technique of the analysis is described in [29].



Table 5: Radioactive contamination of ZnWO<sub>4</sub> scintillators determined by different methods.

Chain	Nuclide	Activity (mBq/kg)	
		ZWO-1	ZWO-2
<sup>232</sup> Th	<sup>232</sup> Th	≤ 0.11 <sup>a</sup>	≤ 0.1 <sup>a</sup>
	<sup>228</sup> Ra	≤ 0.2 <sup>b</sup>	≤ 0.05 <sup>b</sup>
	<sup>228</sup> Th	0.005(3) <sup>c</sup>	0.0015(6) <sup>c</sup>
<sup>235</sup> U	<sup>227</sup> Ac	≤ 0.007 <sup>c</sup>	≤ 0.003 <sup>c</sup>
<sup>238</sup> U	<sup>238</sup> U	≤ 0.1 <sup>a</sup>	≤ 0.08 <sup>a</sup>
	<sup>230</sup> Th	≤ 0.13 <sup>a</sup>	≤ 0.07 <sup>a</sup>
	<sup>226</sup> Ra	≤ 0.006 <sup>a</sup>	0.002(1) <sup>a</sup>
	<sup>210</sup> Po	≤ 0.2 <sup>a</sup>	≤ 0.06 <sup>a</sup>
Total α activity		0.38(5) <sup>a</sup>	0.18(3) <sup>a</sup>
	<sup>40</sup> K	≤ 1 <sup>b</sup>	≤ 0.4 <sup>b</sup>
	<sup>60</sup> Co	≤ 0.05 <sup>b</sup>	≤ 0.1 <sup>b</sup>
	<sup>65</sup> Zn	≤ 0.8 <sup>b</sup>	0.5 <sup>b</sup>
	<sup>87</sup> Rb	1.5 <sup>d</sup> , ≤ 2.6 <sup>b</sup>	3.2 <sup>d</sup> , ≤ 2.3 <sup>b</sup>
	<sup>90</sup> Sr– <sup>90</sup> Y	≤ 0.6 <sup>b</sup>	≤ 0.4 <sup>b</sup>
	<sup>137</sup> Cs	≤ 0.3 <sup>b</sup>	≤ 0.05 <sup>b</sup>
	<sup>147</sup> Sm	≤ 0.01 <sup>a</sup>	≤ 0.01 <sup>a</sup>

<sup>a</sup> Pulse-shape discrimination (see section 3.2)

<sup>b</sup> Fit of background spectra (see section 3.3)

<sup>c</sup> Time-amplitude analysis (see section 3.1)

<sup>d</sup> ICP-MS analysis (see section 2.3)

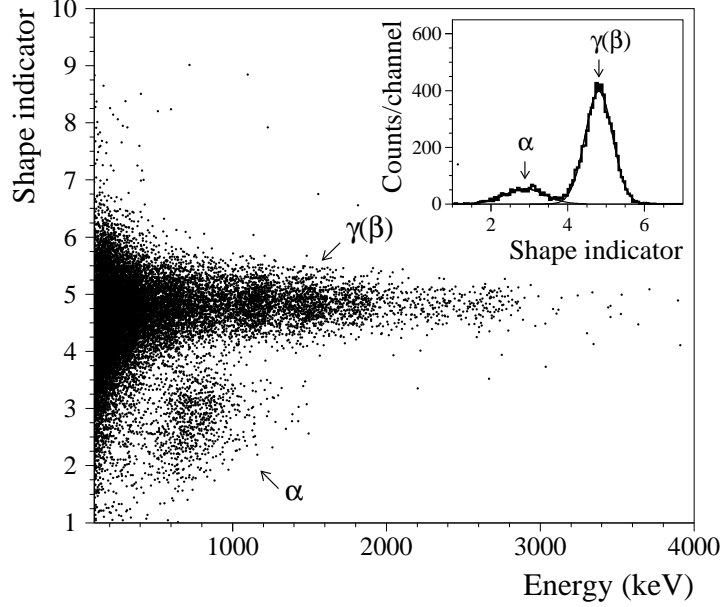


Figure 3: Scatter plot of the shape indicator (see text) versus energy for 2130 h background exposition with the ZWO-2 crystal scintillator (Run 3). (Inset) Distribution of shape indicators for the data selected in the energy interval 0.5–1.0 MeV. Fit of the distribution by two Gaussian functions is shown by solid lines.

be produced from  $^{64}\text{Zn}$  by thermal neutrons (the cross section of  $^{64}\text{Zn}$  to thermal neutrons is 0.76 barn [35]) or/and by cosmogenic activation. There are no other clear peculiarities in the spectra which could be ascribed to the internal trace contamination by radioactive nuclides. Therefore we can obtain only limits on the activities of  $^{40}\text{K}$ ,  $^{60}\text{Co}$ ,  $^{87}\text{Rb}$ ,  $^{90}\text{Sr}$ – $^{90}\text{Y}$ ,  $^{137}\text{Cs}$ , and U/Th daughters (see Table 5). The activity of  $^{65}\text{Zn}$  in the crystal ZWO-2 is at the level of 0.5 mBq/kg. The results of the fit of the spectra (Run 2 and Run 3) in the energy interval 0.1 – 2.9 MeV, and the main components of the background are shown in Fig. 5 and Fig. 6, respectively.

The summary of the measured radioactive contamination of the  $\text{ZnWO}_4$  crystal scintillators (or limits on their activities) is given in Table 5.

It should be stressed that external  $\gamma$  rays contribute the main part of the background of the  $\text{ZnWO}_4$  detectors. For instance  $\approx 90\%$  and  $\approx 70\%$  of the counting rate in the energy interval 0.5 – 1.3 MeV (important to search for the double beta processes in  $^{64}\text{Zn}$ ) are determined by external  $\gamma$  quanta in Run 2 and Run 3, respectively. Therefore one order of magnitude suppression of background of a  $\text{ZnWO}_4$  detector can be reached by improving of the set-up. For this purpose we intend to add two high-purity quartz light-guides 10 cm of length each. Further advancement needs R&D of radiopure  $\text{ZnWO}_4$  scintillators. It should be stressed, no special additional low-radioactive measures were carried out to grow the  $\text{ZnWO}_4$  crystals used in the present experiment. One could assume that the radiopurity of  $\text{ZnWO}_4$  is at some extent an own property of this crystal.

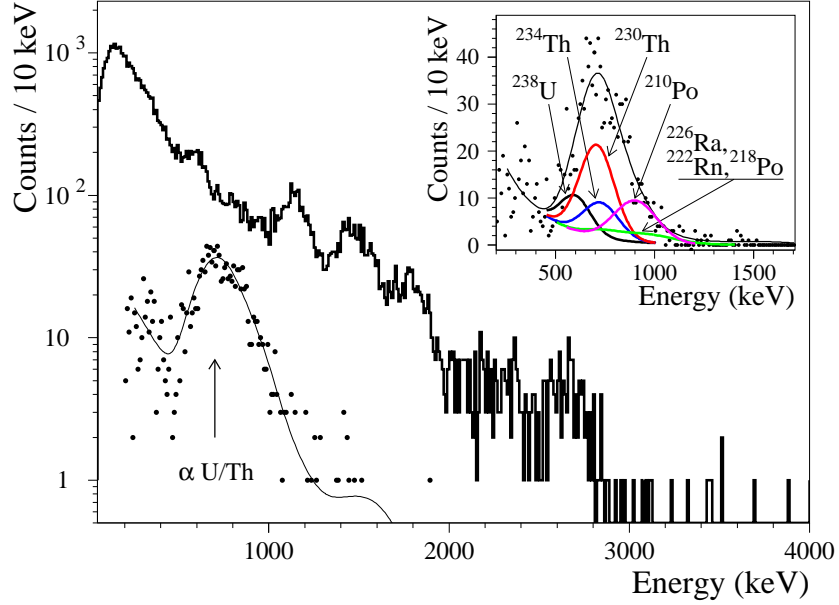


Figure 4: (Color online) The energy spectrum of  $\beta$  particles ( $\gamma$  quanta, solid histogram) and  $\alpha$  particles (dots) selected by the pulse-shape discrimination from raw data measured with the ZWO-2 scintillator during 2130 h (Run 3) in the low background set-up. In the inset, the  $\alpha$  spectrum is depicted together with the model, which includes  $\alpha$  decays from  $^{238}\text{U}$  family. The total  $\alpha$  activity in the  $\text{ZnWO}_4$  crystal is 0.18 mBq/kg.

## 4 Results and discussion

There are no peculiarities in the measured energy spectra of the  $\text{ZnWO}_4$  detectors, which can be interpreted as double beta decay of Zinc or Tungsten isotopes. Therefore only lower half-life limits can be set according to formula:

$$\lim T_{1/2} = N \cdot \eta \cdot t \cdot \ln 2 / \lim S,$$

where  $N$  is the number of potentially  $2\beta$  unstable nuclei,  $\eta$  is the detection efficiency,  $t$  is the measuring time, and  $\lim S$  is the number of events of the effect searched for which can be excluded at given confidence level (C.L.).

The response functions of the  $\text{ZnWO}_4$  detectors for the  $2\beta$  processes searched for and possible background components in each Run with different detectors were simulated with the help of the GEANT4 code [32]. The initial kinematics of the particles emitted in the decays was generated with the DECAY0 event generator [33].

We have used different combinations of data recorded in Runs 1–4 to reach maximal sensitivity to the double beta processes searched for. For instance, the sum of energy spectra measured in Runs 2 and 3 was taken to search for double beta processes in  $^{64}\text{Zn}$  and  $0\nu 2\beta$  decay in  $^{70}\text{Zn}$ , while all the accumulated spectra were used to set limits on the  $2\beta$  decay in  $^{180}\text{W}$ ,  $^{186}\text{W}$ , and  $2\nu 2\beta$  decay in  $^{70}\text{Zn}$  (all these processes have a comparatively low energy release). Response functions for the double beta processes searched for, the components of background describing internal contamination of the crystals, and external  $\gamma$  rays from PMTs were built as sum of models for each Run.

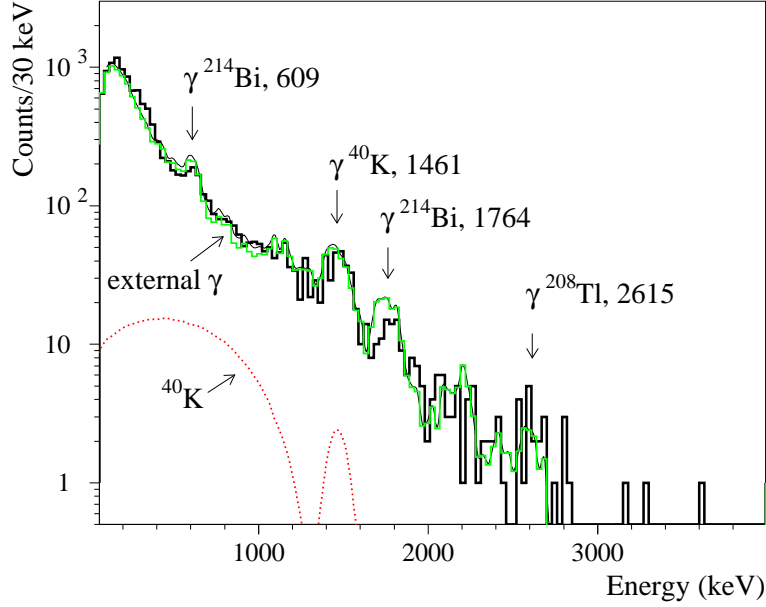


Figure 5: (Color online) Energy spectrum of  $\beta(\gamma)$  events accumulated in the low-background set-up with the ZWO-1 crystal scintillator over 2906 h (Run 2) together with the model of the background. The main components of the background are shown: spectrum of  $^{40}\text{K}$  (internal contamination), and the contribution from the external  $\gamma$  quanta from PMTs in these experimental conditions.

#### 4.1 Search for double electron capture and $\varepsilon\beta^+$ decay of $^{64}\text{Zn}$

The expected energy distributions for the  $2\beta$  processes in the ZWO-2 detector (Run 3) in  $^{64}\text{Zn}$  are shown in Fig. 7. It should be stressed, the registration efficiencies in the whole distributions are at least 99.9% for all the processes.

Two approaches were used to estimate the value of  $\lim S$  for the two neutrino mode of electron capture with positron emission ( $2\nu\varepsilon\beta^+$ ) in  $^{64}\text{Zn}$ . In the first one (the so called  $1\sigma$  approach) statistical uncertainty of the number of events registered in the energy region of the expected peak was taken as  $\lim S$ . 11848 events were observed in the energy interval 490 – 1150 keV of the spectrum Run 2 + Run 3 (see Fig. 8), which gives  $\lim S = 109$  counts. Considering the related efficiency in the energy interval  $\eta = 0.82$ , it gives the half-life limit  $T_{1/2}^{2\nu\varepsilon\beta^+} \geq 1.0 \times 10^{21}$  yr.

In the second approach the energy spectrum was fitted in the energy range 380 – 1430 keV. Background model was composed of  $^{65}\text{Zn}$ ,  $^{90}\text{Sr}-^{90}\text{Y}$ ,  $^{40}\text{K}$ ,  $^{60}\text{Co}$ ,  $^{137}\text{Cs}$ , U/Th inside crystal, and  $^{40}\text{K}$ ,  $^{232}\text{Th}$ ,  $^{238}\text{U}$  in the PMTs. The starting and final energies of fit were varied as 380 – 460 and 1260 – 1430 keV with the step of 10 keV. The fit in the energy region 430 – 1360 keV was chosen as giving the minimal value of  $\chi^2/n.d.f. = 121/80 = 1.51$ . The fit gives total area of the effect  $-232 \pm 235$  counts which corresponds (in accordance with the Feldman-Cousins procedure [36]) to  $\lim S = 192(65)$  counts at 90%(68%) C.L. Taking into account  $\simeq 100\%$  registration efficiency for the whole curve in this case, one can calculate the half-life limit:

$$T_{1/2}^{2\nu\varepsilon\beta^+} (^{64}\text{Zn}) \geq 0.70(2.1) \times 10^{21} \text{ yr at } 90\%(68\%) \text{ C.L.}$$

In the same way the half-life bound on the neutrinoless mode was set as:

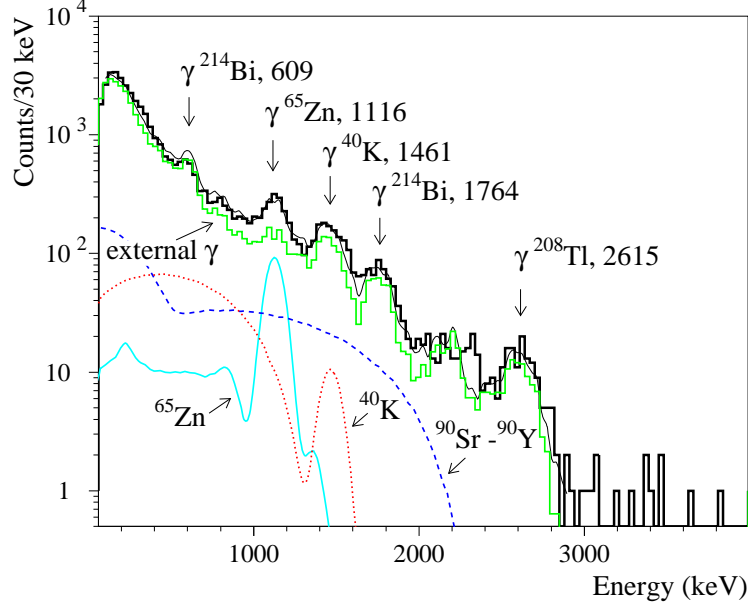


Figure 6: (Color online) Energy spectrum of  $\beta(\gamma)$  events accumulated in the low-background set-up with the ZWO-2 crystal scintillator over 2130 h (Run 3) together with the model of the background. The main components of the background are shown: spectra of  $^{40}\text{K}$ ,  $^{90}\text{Sr}$ – $^{90}\text{Y}$ ,  $^{65}\text{Zn}$ , and the contribution from the external  $\gamma$  quanta from PMTs in these experimental conditions.

$$T_{1/2}^{0\nu\epsilon\beta^+} (^{64}\text{Zn}) \geq 4.3(5.7) \times 10^{20} \text{ yr at } 90\%(68\%) \text{ C.L.}$$

The energy distributions expected for the  $2\nu\epsilon\beta^+$  and  $0\nu\epsilon\beta^+$  decay of  $^{64}\text{Zn}$ , excluded at 90% C.L., are shown in Fig. 8.

In case of  $0\nu 2\epsilon$  decay, different particles are emitted: X rays and Auger electrons from de-excitations in atomic shells, and  $\gamma$  quanta and/or conversion electrons from de-excitation of daughter nucleus. We suppose here that in the nuclear de-excitation process only one  $\gamma$  quantum is emitted that is the most pessimistic scenario from the point of view of registration of such an event in a peak of full absorption at the  $Q_{2\beta}$  energy.  $2K$ ,  $KL$ ,  $2L$  (and other) modes are not energetically resolved in the high energy region because of the finite energy resolution of the detector (see Fig. 7a). Fit of the measured spectrum in the energy interval 430 – 1300 keV gives the following limit:

$$T_{1/2}^{0\nu 2\epsilon} (^{64}\text{Zn}) \geq 1.1(2.8) \times 10^{20} \text{ yr at } 90\%(68\%) \text{ C.L.}$$

All the limits obtained in the present work for the double beta processes in  $^{64}\text{Zn}$ , as well as the results of the most sensitive previous experiments, are presented in Table 6.

## 4.2 Search for $2\beta^-$ decay of $^{186}\text{W}$ and $^{70}\text{Zn}$

The expected energy spectra for different channels of  $2\beta$  decay of  $^{186}\text{W}$  are shown in Inset of Fig. 9.

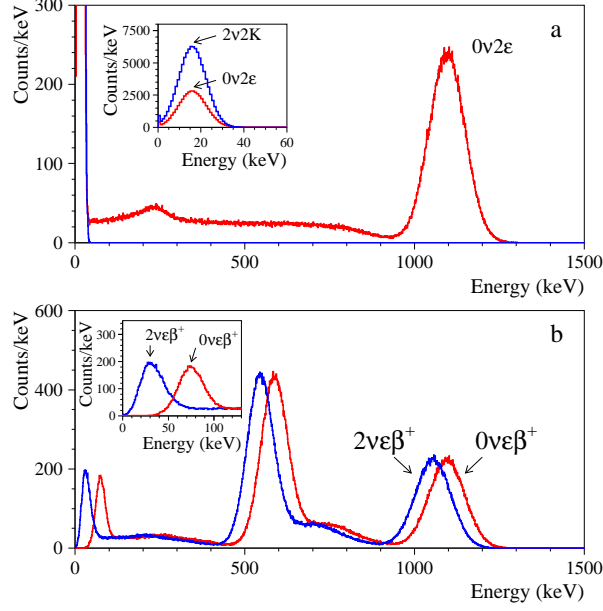


Figure 7: (Color online) Simulated response functions of the  $\text{ZnWO}_4$  scintillator (ZWO-2) for two neutrino and neutrinoless  $2\varepsilon$  (a) and  $\varepsilon\beta^+$  (b) decays in  $^{64}\text{Zn}$ . One million of decays was simulated for each mode.

The energy spectrum Run 1 + Run 2 + Run 3 + Run 4 was used to search for  $2\beta^-$  decays of  $^{186}\text{W}$  to the ground state and to the first excited ( $2_1^+$ ) level of  $^{186}\text{Os}$  ( $E_{exc} = 137$  keV). "One sigma" approach gives the same limit  $T_{1/2}^{0\nu 2\beta} \geq 1.1 \times 10^{21}$  yr for both transitions (because of practically the same registration efficiencies:  $\eta = 99.2\%$  and  $\eta = 97.6\%$  in the energy interval 400 – 600 keV for transitions to the ground and to the excited states, respectively). Fit in the energy interval 380 – 620 keV gives the limit at 90%(68%) C.L.:

$$T_{1/2}^{0\nu 2\beta} (^{186}\text{W}, \text{g.s. and } 2_1^+) \geq 2.1(4.2) \times 10^{20} \text{ yr.}$$

Fit of the spectra accumulated in Run 3 in the energy interval 190 – 450 keV allows to set the limit on the  $0\nu 2\beta$  decay with Majoron emission:

$$T_{1/2}^{0\nu 2\beta M1} (^{186}\text{W}, \text{g.s.}) \geq 5.8(8.6) \times 10^{19} \text{ yr.}$$

The best sensitivity to the two neutrino mode of  $2\beta$  decay of  $^{186}\text{W}$  was achieved with the spectrum obtained by sum of Runs 3 and 4 (see Fig. 9). Fit in the energy interval 70 – 450 keV gives the number of events  $2037 \pm 1125$  which corresponds to  $\text{lim } S = 3882(3162)$ . It allows to set the half-life limit:

$$T_{1/2}^{2\nu 2\beta} (^{186}\text{W}, \text{g.s.}) \geq 2.3(2.8) \times 10^{19} \text{ yr.}$$

Fit of the spectrum (Run 1 + Run 2 + Run 3 + Run 4) in the energy interval 190 – 450 keV gives the following restriction for the half-life relatively to the  $2\nu 2\beta$  decay of  $^{186}\text{W}$  to the first excited level  $2_1^+$  of  $^{186}\text{Os}$ :

$$T_{1/2}^{2\nu 2\beta} (^{186}\text{W}, 2_1^+) \geq 1.8(3.6) \times 10^{20} \text{ yr.}$$

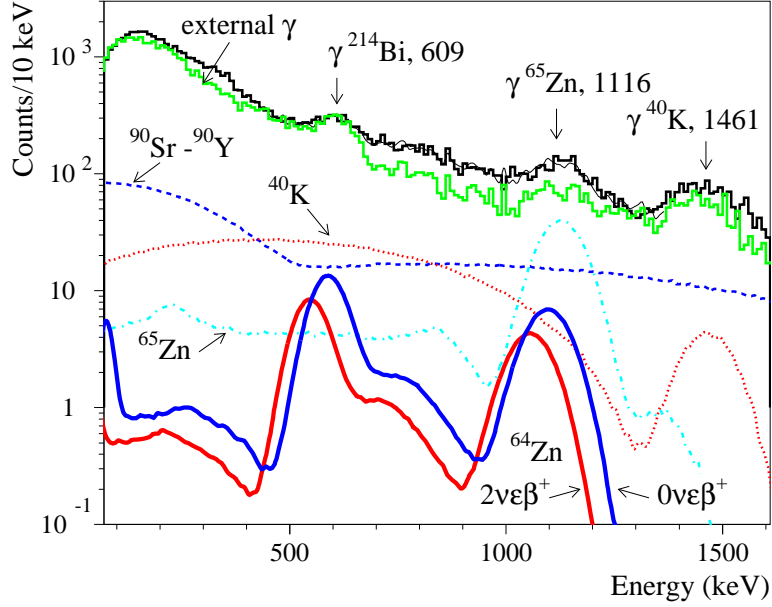


Figure 8: (Color online) The measured energy spectrum of  $\text{ZnWO}_4$  scintillation crystals (Run 2 + Run 3) together with the response functions for  $\varepsilon\beta^+$  process in  $^{64}\text{Zn}$  excluded at 90% C.L. Most important components of the background are shown. The energies of  $\gamma$  lines are in keV.

Similarly, the limits on  $2\beta^-$  processes in  $^{70}\text{Zn}$  were obtained.

All the results are listed in Table 6 where the best previous limits are also given for comparison. The limits obtained for neutrinoless modes of  $2\beta$  decay of  $^{186}\text{W}$  are on the level of the existing results, while the restrictions for the two neutrino models of  $2\beta$  decay in  $^{186}\text{W}$ , and the results for  $^{70}\text{Zn}$  were improved by one order of magnitude. The bound on the  $0\nu 2\beta$  decay of  $^{70}\text{Zn}$  with Majoron emission was set for the first time.

It is important to note that in accordance with theoretical calculations in the pseudo  $\text{SU}(3)$  framework [37] which take into account deformation of the  $^{186}\text{W}$  nucleus (in contrast with the standard QRPA method), the  $2\nu 2\beta$  decay rate of  $^{186}\text{W}$  could be strongly suppressed (up to being equal to 0). Hence, the energy region of  $0\nu 2\beta$  signal of  $^{186}\text{W}$  will be free of the background created by the  $2\nu 2\beta$  events, which can reach this region due to the poor energy resolution of the detector. The suppression of the  $2\nu$  mode would be especially important in the search for the  $0\nu$  decay with Majoron emission, whose distribution is continuous, because in this case the  $0\nu 2\beta M1$  events will not be distinguished from the  $2\nu$  background even with the help of the high energy resolution detector.

### 4.3 $2\varepsilon$ capture in $^{180}\text{W}$

To set the limits on the  $0\nu 2\varepsilon$  process in  $^{180}\text{W}$ , the sum of the background spectra of  $\text{ZnWO}_4$  detectors accumulated in all four Runs was used (the low energy part of the spectrum is shown in Fig. 10). The least squares fit of this spectrum in the 70–270 keV energy interval gives  $133 \pm 256$  counts for the  $0\nu 2\varepsilon$  peak searched for ( $\chi^2/n.d.f. = 12.8/7 = 1.83$ ), providing no evidence for the effect. These numbers lead to an upper limit of 553(389) counts at 90%(68%) C.L. Taking into account registration efficiency for this process close to 1, one can calculate the half-life limit:

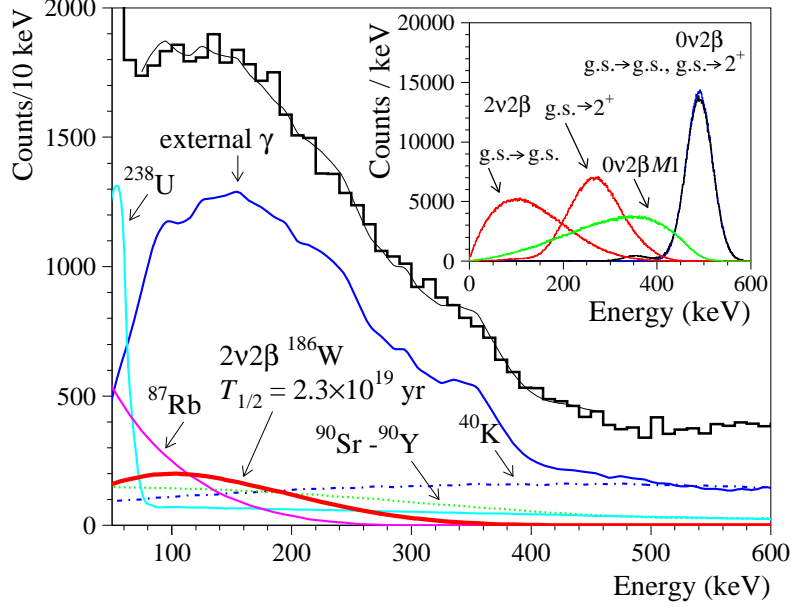


Figure 9: (Color online) Energy spectrum of background obtained by sum of Runs 3 and 4 together with fit and main components of the background (external  $\gamma$  ray from PMT, internal  $^{40}\text{K}$ ,  $^{87}\text{Rb}$ ,  $^{90}\text{Y}$ - $^{90}\text{Sr}$ ,  $^{238}\text{U}$ ). The simulated response function for  $2\nu 2\beta$  decay of  $^{186}\text{W}$  with the half-life  $T_{1/2}^{2\nu 2\beta} = 2.3 \times 10^{19}$  excluded at 68% is also shown. (Inset) Simulated response functions for different double beta processes in  $^{186}\text{W}$ . The distribution for  $0\nu 2\beta$  decay to the ground state of  $^{186}\text{Os}$  is practically indistinguishable from the peak of  $0\nu 2\beta$  decay to the  $2^+$  excited state of  $^{186}\text{Os}$ .

$$T_{1/2}^{0\nu 2\varepsilon}(^{180}\text{W}) \geq 0.86(1.2) \times 10^{18} \text{ yr.}$$

The same method gives the restriction for the  $2\nu 2K$  process in  $^{180}\text{W}$ :

$$T_{1/2}^{2\nu 2K}(^{180}\text{W}) \geq 6.6(9.4) \times 10^{17} \text{ yr.}$$

The obtained limits are one order of magnitude better than the previous limits obtained in the work [18] by using enriched in  $^{116}\text{Cd}$  cadmium tungstate crystal scintillators. The improvement is reached thanks to absence of the  $\beta$  active  $^{113}\text{Cd}$  ( $Q_\beta = 320$  keV [11],  $T_{1/2} = 8.04 \times 10^{15}$  yr [38]) in  $\text{ZnWO}_4$  scintillators providing the main background in the  $^{116}\text{CdWO}_4$  detectors at low energy. The response functions for  $0\nu 2\varepsilon$  and  $2\nu 2K$  decay of  $^{180}\text{W}$  corresponding to the limits obtained in the work [18] are presented in Fig. 10.

All the half-life limits on  $2\beta$  decay processes in Zinc and Tungsten obtained in the present experiment are summarized in Table 6 where results of the most sensitive previous experiments are given for comparison.

All the obtained half-life bounds are well below the existing theoretical predictions [39, 40]; nevertheless most of the limits are near one orders of magnitude higher than those established in previous experiments. It should be stressed that only a few nuclei among potentially  $2\varepsilon$ ,  $\varepsilon\beta^+$ ,  $2\beta^+$  active isotopes were investigated at the level of sensitivity  $\sim 10^{21}$  yr.

Further improvement of sensitivity can be reached by increasing of mass of the  $\text{ZnWO}_4$  detector, suppression of external background, development of  $\text{ZnWO}_4$  scintillators with lower level of radioactive contamination.



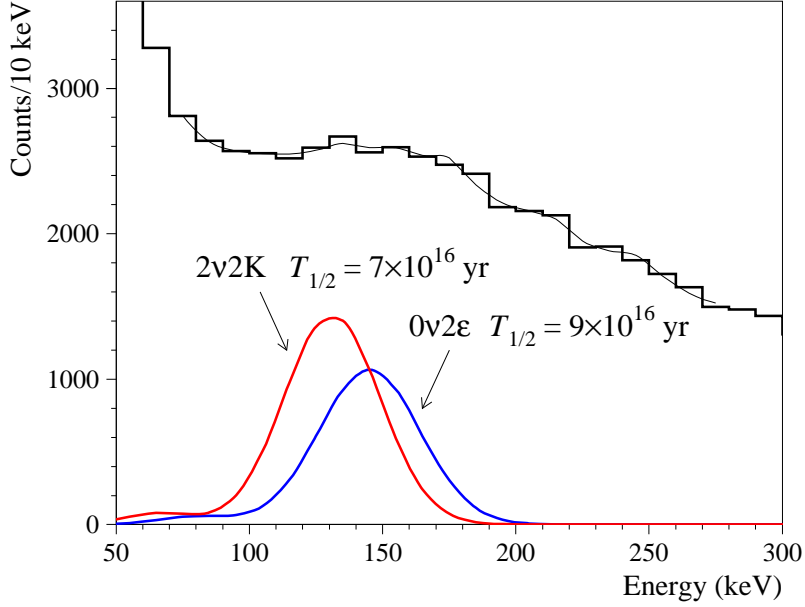


Figure 10: (Color online) Energy spectrum of background obtained by sum of Runs 1 – 4 together with fit in the energy interval 70–270 keV. The simulated response functions for double electron capture in  $^{180}\text{W}$  are shown; the half-lives  $T_{1/2}^{2\nu 2K} = 7 \times 10^{16}$  yr and  $T_{1/2}^{0\nu 2\varepsilon} = 9 \times 10^{16}$  yr correspond to the the best previous limits reported in [18].

## 5 Conclusions

Low background experiment to search for  $2\beta$  processes in  $^{64}\text{Zn}$ ,  $^{70}\text{Zn}$ ,  $^{180}\text{W}$ ,  $^{186}\text{W}$  was carried out over more than 10 thousands hours in the underground Gran Sasso National Laboratories of INFN by using large volume (117 g, 168 g, and 699 g) low-background  $\text{ZnWO}_4$  crystal scintillators.

The new improved half-life limits on double electron capture and electron capture with positron emission in  $^{64}\text{Zn}$  have been set, in particular (all the limits are at 90% C.L.):  $T_{1/2}^{0\nu 2\varepsilon} \geq 1.1 \times 10^{20}$  yr,  $T_{1/2}^{2\nu \varepsilon \beta^+} \geq 0.70 \times 10^{21}$  yr, and  $T_{1/2}^{0\nu \varepsilon \beta^+} \geq 4.3 \times 10^{20}$  yr. The positive indication on the  $(2\nu + 0\nu)\varepsilon\beta^+$  decay of  $^{64}\text{Zn}$  with  $T_{1/2} = (1.1 \pm 0.9) \times 10^{19}$  yr suggested in [13] is fully discarded by the present experiment. To date only three nuclei ( $^{40}\text{Ca}$ ,  $^{78}\text{Kr}$ , and  $^{106}\text{Cd}$ ) were studied at the similar level of sensitivity ( $T_{1/2} \sim 10^{21}$  yr). However, it is worth noting that the theoretical predictions are still higher.

The half-life limits on the  $2\beta$  processes in  $^{70}\text{Zn}$ ,  $^{180}\text{W}$ , and two neutrino mode of  $2\beta$  decay in  $^{186}\text{W}$  established in our work on the level of  $10^{18} - 10^{20}$  yr are one order of magnitude higher than those of previous experiments.

We have found  $\text{ZnWO}_4$  crystal scintillators extremely radiopure detectors with typical contamination at the level of  $\mu\text{Bq/kg}$  ( $^{228}\text{Th}$  and  $^{226}\text{Ra}$ ),  $\leq 0.06$  mBq/kg ( $^{210}\text{Po}$ ), total activity (U/Th) 0.2–0.4 mBq/kg,  $\leq 0.4$  mBq/kg ( $^{40}\text{K}$ ),  $\leq 0.05$  mBq/kg ( $^{137}\text{Cs}$ ),  $\leq 0.4$  mBq/kg ( $^{90}\text{Sr}$ – $^{90}\text{Y}$ ),  $\leq 0.01$  mBq/kg ( $^{147}\text{Sm}$ ), and  $\leq 3$  mBq/kg ( $^{87}\text{Rb}$ ).

An experiment involving  $\approx 10$  tons of *nonenriched* crystals ( $9 \times 10^{27}$  nuclei of  $^{64}\text{Zn}$ ) could reach the half-life sensitivity  $\sim 4 \times 10^{28}$  yr (supposing zero background during ten years of measurements). Such a sensitivity could contribute to our understanding of the neutrino mass

Table 6: Half-life limits on  $2\beta$  processes in Zn and W isotopes.

Transition	Decay channel	Level of daughter nucleus	$T_{1/2}$ limit (yr)	
			Present work 90%(68%) C.L.	Previous results 90%(68%) C.L.
$^{64}\text{Zn} \rightarrow ^{64}\text{Ni}$	$0\nu 2\varepsilon$	g.s.	$\geq 1.1(2.8) \times 10^{20}$	$\geq 0.7(1.0) \times 10^{18}$ [15] $\geq 3.4(5.5) \times 10^{18}$ [17]
	$0\nu \varepsilon \beta^+$	g.s.	$\geq 4.3(5.7) \times 10^{20}$	$\geq 2.8 \times 10^{16}$ [14] $\geq 2.4(3.6) \times 10^{18}$ [15] $\geq 1.3 \times 10^{20}$ [16]
	$2\nu \varepsilon \beta^+$	g.s.	$\geq 0.70(2.1) \times 10^{21}$	$\geq 2.2(6.1) \times 10^{20}$ [17] $= (1.1 \pm 0.9) \times 10^{19}$ [13] $\geq 4.3(8.9) \times 10^{18}$ [15] $\geq 1.3 \times 10^{20}$ [16] $\geq 2.1(7.4) \times 10^{20}$ [17]
$^{70}\text{Zn} \rightarrow ^{70}\text{Ge}$	$0\nu 2\beta^-$	g.s.	$\geq 1.8(3.0) \times 10^{19}$	$\geq 0.7(1.4) \times 10^{18}$ [15]
	$2\nu 2\beta^-$	g.s.	$\geq 2.3(4.0) \times 10^{17}$	$\geq 1.3(2.1) \times 10^{16}$ [15]
	$0\nu 2\beta^- \text{M1}$	g.s.	$\geq 1.0(1.4) \times 10^{18}$	
$^{180}\text{W} \rightarrow ^{180}\text{Hf}$	$0\nu 2\varepsilon$	g.s.	$\geq 0.86(1.2) \times 10^{18}$	$\geq 0.9(1.3) \times 10^{17}$ [18]
	$2\nu 2K$	g.s.	$\geq 6.6(9.4) \times 10^{17}$	$\geq 0.7(0.8) \times 10^{17}$ [18]
$^{186}\text{W} \rightarrow ^{186}\text{Os}$	$0\nu 2\beta^-$	g.s.	$\geq 2.1(4.2) \times 10^{20}$	$\geq 1.1(2.1) \times 10^{21}$ [18]
	$0\nu 2\beta^-$	$2^+$ (137.2 keV)	$\geq 2.1(4.2) \times 10^{20}$	$\geq 1.1(2.0) \times 10^{21}$ [18]
	$0\nu 2\beta^- \text{M1}$	g.s.	$\geq 5.8(8.6) \times 10^{19}$	$\geq 1.2(1.4) \times 10^{20}$ [18]
	$2\nu 2\beta^-$	g.s.	$\geq 2.3(2.8) \times 10^{19}$	$\geq 3.7(5.3) \times 10^{18}$ [18]
	$2\nu 2\beta^-$	$2^+$ (137.2 keV)	$\geq 1.8(3.6) \times 10^{20}$	$\geq 1.0(1.3) \times 10^{19}$ [18]

mechanism and right-handed currents in neutrinoless processes [10]. As well, two neutrino double electron capture should be surely observed: in accordance with theoretical expectations [39, 40],  $T_{1/2}$  for  $2\nu 2\varepsilon$  process is predicted on the level of  $10^{25} - 10^{26}$  yr.

## 6 Acknowledgments

The group from the Institute for Nuclear Research (Kyiv, Ukraine) was supported in part by the Project "Kosmomikrofizyka" (Astroparticle Physics) of the National Academy of Sciences of Ukraine.

## References

- [1] V.I. Tretyak, Yu.G. Zdesenko, At. Data Nucl. Data Tables 61 (1995) 43; 80 (2002) 83.
- [2] Yu.G. Zdesenko, Rev. Mod. Phys. 74 (2002) 663.
- [3] J.D. Vergados, Phys. Rept. 361 (2002) 1.

- [4] S.R. Elliot, P. Vogel, *Ann. Rev. Nucl. Part. Sci.* 52 (2002) 115.
- [5] S.R. Elliot, J. Engel, *J. Phys. G: Nucl. Part. Phys.* 30 (2004) R183.
- [6] A.S. Barabash, *Phys. At. Nucl.* 67 (2004) 438.
- [7] F.T. Avignone III, G.S. King, Yu.G. Zdesenko, *New J. Phys.* 7 (2005) 6.
- [8] H. Ejiri, *J. Phys. Soc. Japan* 74 (2005) 2101.
- [9] F.T. Avignone III, S.R. Elliott, J. Engel, *Rev. Mod. Phys.* 80 (2008) 481.
- [10] M. Hirsch et al., *Z. Phys. A* 347 (1994) 151.
- [11] G. Audi, A.H. Wapstra, C. Thibault, *Nucl. Phys. A* 729 (2003) 337.
- [12] J.K. Bohlke et al., *J. Phys. Chem. Ref. Data* 34 (2005) 57.
- [13] I. Bikit et al., *Appl. Radiat. Isot.* 46 (1995) 455.
- [14] H. Kiel et al., *Nucl. Phys. A* 723 (2003) 499.
- [15] F.A. Danevich et al., *Nucl. Instr. Meth. A* 544 (2005) 553.
- [16] H.J. Kim et al., *Nucl. Phys. A* 793 (2007) 171.
- [17] P. Belli et al., *Phys. Lett. B* 658 (2008) 193.
- [18] F.A. Danevich et al., *Phys. Rev. C* 68 (2003) 035501.
- [19] L.L. Nagornaya et al., *IEEE Trans. Nucl. Sci.* 55 (2008) 1.
- [20] L.L. Nagornaya et al., Large volume ZnWO<sub>4</sub> crystal scintillator with excellent energy resolution and low background, presented on 2008 Symp. on Radiation Measurements and Applications (SORMA WEST 2008), June 2-5, 2008, Berkeley, California, USA.
- [21] F.A. Danevich et al., *Phys. Lett. B* 344 (1995) 72.
- [22] F.A. Danevich et al., *Nucl. Phys. A* 694 (2001) 375.
- [23] E. Gatti, F. De Martini, *Nuclear Electronics 2*, IAEA, Vienna, 1962, p. 265.
- [24] T. Fazzini et al., *Nucl. Instr. Meth. A* 410 (1998) 213.
- [25] L. Bardelli et al., *Nucl. Instr. Meth. A* 569 (2006) 743.
- [26] P. Belli et al., *Nucl. Instr. Meth. A* 498 (2003) 352.
- [27] Yu.G. Zdesenko et al., *Nucl. Instrum. Meth. A* 538 (2005) 657.
- [28] F.A. Danevich et al., *Nucl. Instr. Meth. A* 541 (2005) 583.
- [29] P. Belli et al., *Nucl. Phys. A* 789 (2007) 15.

- [30] L. Bardelli et al., Nucl. Instr. Meth. A 584 (2008) 129.
- [31] A.N. Annenkov et al., Nucl. Instr. Meth. A 584 (2008) 334.
- [32] S. Agostinelli et al., Nucl. Instr. Meth. A 506 (2003) 250;  
J. Allison et al., IEEE Trans. Nucl. Sci. 53 (2006) 270.
- [33] O.A. Ponkratenko et al., Phys. At. Nucl. 63 (2000) 1282;  
V.I. Tretyak, to be published.
- [34] R. Bernabei et al., Il Nuovo Cim. A 112 (1999) 545.
- [35] R.B. Firestone, S.Y. Frank Chu, C.M. Baglin, Table of Isotopes, 8th ed., CD 1998 Update,  
Lawrence Berkeley National Laboratory, University of California.
- [36] G.J. Feldman, R.D. Cousins, Phys. Rev. D 57 (1998) 3873.
- [37] O. Castanos, J.G. Hirsch, O. Civitarese, P.O. Hess, Nucl. Phys. A 571 (1994) 276.
- [38] P. Belli et al., Phys. Rev. C 76 (2007) 064603.
- [39] P. Domin, S. Kovalenko, F. Simkovic, S.V. Semenov, Nucl. Phys. A 753 (2005) 337.
- [40] E.-W. Grewe et al., Phys. Rev. C 77 (2008) 064303.